



HAL
open science

Metal/ceramic composites from freeze-cast ceramic preforms: Domain structure and elastic properties

Siddhartha Roy, Alexander Wanner

► **To cite this version:**

Siddhartha Roy, Alexander Wanner. Metal/ceramic composites from freeze-cast ceramic preforms: Domain structure and elastic properties. *Composites Science and Technology*, 2009, 68 (5), pp.1136. 10.1016/j.compscitech.2007.06.013 . hal-00534152

HAL Id: hal-00534152

<https://hal.science/hal-00534152>

Submitted on 9 Nov 2010

HAL is a multi-disciplinary open access archive for the deposit and dissemination of scientific research documents, whether they are published or not. The documents may come from teaching and research institutions in France or abroad, or from public or private research centers.

L'archive ouverte pluridisciplinaire **HAL**, est destinée au dépôt et à la diffusion de documents scientifiques de niveau recherche, publiés ou non, émanant des établissements d'enseignement et de recherche français ou étrangers, des laboratoires publics ou privés.

Accepted Manuscript

Metal/ceramic composites from freeze-cast ceramic preforms: Domain structure and elastic properties

Siddhartha Roy, Alexander Wanner

PII: S0266-3538(07)00261-8
DOI: [10.1016/j.compscitech.2007.06.013](https://doi.org/10.1016/j.compscitech.2007.06.013)
Reference: CSTE 3752

To appear in: *Composites Science and Technology*

Received Date: 15 March 2007
Revised Date: 17 June 2007
Accepted Date: 19 June 2007

Please cite this article as: Roy, S., Wanner, A., Metal/ceramic composites from freeze-cast ceramic preforms: Domain structure and elastic properties, *Composites Science and Technology* (2007), doi: [10.1016/j.compscitech.2007.06.013](https://doi.org/10.1016/j.compscitech.2007.06.013)

This is a PDF file of an unedited manuscript that has been accepted for publication. As a service to our customers we are providing this early version of the manuscript. The manuscript will undergo copyediting, typesetting, and review of the resulting proof before it is published in its final form. Please note that during the production process errors may be discovered which could affect the content, and all legal disclaimers that apply to the journal pertain.



Metal/ceramic composites from freeze-cast ceramic preforms:**Domain structure and elastic properties**

Siddhartha Roy & Alexander Wanner

Institut für Werkstoffkunde I, Universität Karlsruhe (TH), Kaiserstr. 12,

76131 Karlsruhe, Germany

Keywords: Metal matrix composites, mechanical properties, anisotropy, elastic properties, ultrasonics.

Abstract: Innovative metal/ceramic composites produced by melt infiltration of ceramic preforms prepared by a freeze casting technique are examined in this study. These composites exhibit a characteristic hierarchical structure: On a mesoscopic length scale, lamellar domains with sizes up to several millimetres are observed. The aim of the present study was to analyze the anisotropic elastic properties of such a composite on different length scales. Experimental studies were carried out on samples containing about 44% alumina ceramic and 56% aluminium-based alloy (Al-12Si). Ultrasonic wave velocity measurements were carried out on macroscopic poly-domain samples as well as on miniature single-domain samples. The elastic constants derived from these measurements are discussed in light of elasticity models established for lamellar and for fibrous composites.

1. Introduction

In the past decades, a variety of metal matrix composites have been developed and introduced into numerous engineering applications [1, 2, 3, 4]. There is, however, still room for further development in the directions of novel property profiles and more efficient and economic processing techniques. New perspectives have recently been opened by the availability of innovative ceramic preform materials produced by freeze-casting of ceramic suspensions. For details about this processing route we refer to Refs. [5, 6, 7, 8, 9]. The porous ceramic bodies produced this way exhibit excellent permeability for gases and liquids in combination with acceptable mechanical strengths [5]. Preforms produced from water-based slurries typically exhibit a hierarchical structure in which lamellar domains play an important role. The lamellar structure is a result of the growth morphology of the ice crystals formed during freeze-casting. The size and internal structure of the domains can be controlled via the freeze casting parameters [5, 8]. Porous ceramics of this kind are of potential interest for a number of applications and as has been shown by Mattern [5] and Deville et al. [10, 11], they appear to be specifically suited as preform material for the production of metal matrix composites via squeeze-casting or even die-casting [12, 13] with reinforcement content in the range from 30 to 70 volume pct. This is of particular interest since conventional particle- or fiber-reinforced MMCs typically exhibit either a relatively low (5-30 vol. pct, e.g. [14]) or a fairly high (50-80 vol. pct., e.g. [15, 16]) reinforcement content due to processing constraints.

In the present study, a first account of the elastic properties of such an innovative MMC is given. The elastic behavior is characterized on different length scales by characterizing samples of different size by means of a special ultrasonic spectroscopy

technique. This way for the first time insight into the elastic anisotropy on domain level is obtained. The implications for the interaction between adjacent domains and for the macroscopic mechanical behaviour of such composites will be discussed.

2. Experimental procedure

2.1. Specimen materials

Two types of alumina preforms with porosities of about 56 vol. pct. were produced at Institut für Keramik im Maschinenbau (IKM) at Universität Karlsruhe, Karlsruhe, Germany, via freeze-casting of a ceramic suspension and subsequent sintering. Water was used as the liquid vehicle during freeze-casting and the suspension contained 22 vol% of alumina powder (CT3000SG from Almatis with nominal alumina content of 99.8%, powder particle size 2.5 μm / D90 Cilas and a fired density of 3.90 Mg/m^3), 0.5 wt% Dolapix CE64 as dispersant and 10 wt% Optapix PAF60 as a binder. The freeze-casting temperature was either -10°C (Type A) or -30°C (Type B). Freeze cast ceramic preforms were sintered at 1550°C for 1 hour. Afterwards they were brought to room temperature at a cooling rate of $4^\circ\text{C}/\text{min}$. Preforms with nominal dimensions $10 \times 44 \times 66 \text{ mm}^3$ were infiltrated with a eutectic aluminum-silicon alloy (Al-12Si) at the Casting Technology Center at Aalen University of Applied Sciences, Aalen, Germany, using a squeeze-casting technique. Before squeeze casting the preforms were preheated to 800°C and the press was heated upto 400°C .

In Figures 1 (a) and (b) typical metallographic sections of the two MMC types are shown. In these light-optical micrographs, the ceramic component appears dark and the metal matrix appears bright. The sections are oriented perpendicular to the freezing direction used during preform fabrication. For MMC Type A (Figure 1(a)) a quite

coarse structure is observed, exhibiting lamellar domains with sizes up to several millimetres. The material appears fully dense but exhibits some matrix rich regions which are due to the unwanted removal of individual ceramic lamellae during the grinding of the preform prior to metal infiltration. Such matrix-rich regions are therefore only observed near the surface of the MMC and have no significant effect on the bulk properties. In comparison, the MMC Type B (Figure 1(b)) has a much finer structure. The domains are considerably smaller and the lamellae are much thinner. According to the discussions of Deville et al. [10, 11], this follows directly from the lower freezing temperature of the ceramic preforms of MMC Type B. The lower freezing temperature generated a higher freezing rate and consequently the extent of supercooling ahead of the solidifying front increased, reducing the tip radius of the growing ice crystals. In Figures 2 (a-d) sections parallel to the freeze-casting direction are shown for both MMC types. It can be seen that the lamellae are predominantly oriented parallel to the freeze-casting direction and stretch over the whole thickness of the MMC plate. In these “side views”, the lamellae appear much thicker and more widely spaced compared to the perpendicular sections because the lamellae are sectioned in a random fashion. The partly irregular patterns, marked with arrows in Figures 2b and 2c, indicate that the lamellae are neither perfectly planar nor perfectly aligned parallel to the macroscopic direction of heat removal.

For ultrasonic characterization of elastic properties, rectangular parallelepiped samples were produced from the MMC plates via cutting and grinding. The edges of these parallelepipeds were always parallel to the edges of the MMC plates. In the following, the specimen coordinate system depicted in Figure 3 is used, where direction 1 is the freeze-casting direction. For MMC Type A, samples of two size classes were

produced: 27 relatively large samples with edge lengths in the range from 6 to 10 millimetres, which can be considered to be quasi-homogeneous, poly-domain aggregates like the one sketched in Figure 3, as well as a number of relatively small samples with edge lengths in the range from 1.8 to 2.5 millimetres, consisting of one or two domains having arbitrary lamellae orientations in the 2-3 plane. These smaller samples were produced by wire cutting, using 220 μm thick diamond-coated steel wire. Out of these smaller samples twelve were chosen, which had single domains extending over the whole volume. As is apparent from Figure 4, the lamellae are fairly parallel over the whole sample and their orientation can be described by the angle α (angle between lamellae and specimen axis 2).

For MMC Type B only 30 relatively large, poly-domain samples were produced because single-domain samples of this type of material would not be feasible for our experiments.

In Table 1 the average of the densities deduced from the dimensions and masses of all samples within a MMC type are shown. On average, the density of MMC Type A is slightly lower than that of MMC Type B (3.12 Mg m^{-3} and 3.18 Mg m^{-3} , respectively).

2.2. Wave velocity determination by phase comparison

It is a standard approach to determine elastic constants from the velocities of elastic waves propagating through the material of interest [17]. Ultrasonic Phase Spectroscopy (UPS) is a viable technique to determine wave velocities on samples exhibiting large attenuations due to scattering or internal friction [18, 19, 20, 21]. Continuous, sinusoidal elastic waves are used for the measurements and the phase shift

occurring as the wave passes through the specimen is recorded as a function of frequency. For details about this technique we refer to Ref. [18]. In the present study, the measurements were accomplished using an electronic network analyser (Advantest, model R3754A) and two identical broadband ultrasonic longitudinal-wave transducers (Panametrics, model V122) with nominal central frequency 7.5 MHz and diameter 9.5 mm. These transducers were attached on opposite sides of the rectangular parallelepiped samples with the help of a water soluble couplant. The phase and amplitude spectra were recorded in the frequency range from 10 kHz to 15 MHz. Examples of phase and amplitude spectra obtained on a single-domain sample and one poly-domain sample of MMC Type A are shown in Figure 5. In a non-dispersive medium, the velocity V of a wave propagating through a body of length L can be determined from the slope m of a straight line fitted to the phase vs. frequency spectrum according to the equation [18, 19, 21]

$$V = -2\pi \frac{L}{m} \quad (\text{Eq. 1})$$

In the present work this slope was found to be fairly constant over a considerable frequency range for all of the measurements, indicating that the velocity is in fact independent of frequency (absence of dispersion) and suggesting that elastic constants computed based on the ultrasonic velocities can be assumed to be valid also under static loading conditions. The wave velocity measurements were carried out along the three orthogonal specimen axes for all rectangular specimens described above.

3. Results and discussion

In Table 1 velocities V_1 , V_2 and V_3 measured for propagation of longitudinal waves along the three principal specimen directions 1, 2, and 3, respectively, averaged over all the specimens within a MMC type are listed. The results obtained for the poly-domain samples are also plotted against the density in Figures 6 and 7. The experimental observations can be summarized as follows:

- The velocity V_1 (propagation parallel to the freeze-casting direction) is generally higher than the velocities V_2 and V_3 (propagation along a transverse direction), indicating that the stiffness is highest along the freezing direction.
- Except for very few results, V_1 appears to be strongly correlated to the density. Two non-distinguishable effects may contribute to this: both an increased ceramic content and a low porosity are expected to increase the density as well as the velocity.
- For both MMC Type A and Type B, the transverse velocities V_2 and V_3 exhibit significant scatter which is not correlated to the density. For intermediate ceramic content, the dependence of transverse velocity on the density should be inherently low. The enormous scatter observed in our study is probably due to the presence of closed cracks in the microstructure since such cracks do affect the stiffness and the wave velocity but have little effect on the density. An example of a closed crack is shown in Figure 8. This micrograph shows a single-domain sample of MMC Type A exhibiting a large crack (data points marked within the parentheses in Figure 10). Obviously such cracks exist but are rare enough to affect each sample in a different manner.

- The single-domain specimens show a more pronounced scatter in their properties, due to the small probed volume and due to the pronounced orientations of the lamellae.

Results obtained from individual samples showed that the difference between the two transverse velocities (V_2 and V_3) is relatively higher for MMC Type A. This follows from the larger domain size in this MMC type, as a result of which the individual samples do not cover representative volumes. Table 1 shows that the averages of V_2 and V_3 within a particular MMC type are not significantly different taking the standard deviations into consideration. Hence, transverse isotropy has been assumed on a macroscopic length scale. Denoting the longitudinal wave velocity along principal direction “ i ” by “ V_i ”, the elastic constant for that direction can be calculated according to [18]

$$C_{ii} = \rho V_i^2 \quad (i = 1, 2, 3) \quad (\text{Eq. 2})$$

where ρ is the density. These constants were determined for each individual sample. In Table 1 the stiffness constants obtained by averaging over samples of the MMC type are summarized, assuming transverse isotropy.

In Figure 9 these elastic coefficients are compared to the boundaries as predicted based on the transverse isotropic models for unidirectional fiber-reinforced composites compiled by Berthelot [Eqn. 9.30 in 22]. A more rigorous model should take into consideration the elastic properties of the single domains and then compute the effective properties of polydomain aggregates based on their orientation. Still, for a first estimation, the unidirectional fiber model has been used in this study. For the computation of the theoretical fiber model, the Young’s modulus, density and Poisson’s

ratio of alumina were taken as 390 GPa, 3.9 Mg/m³ [23] and 0.24 [24] respectively. The density, Young's modulus and shear modulus of Al-12Si were measured in this study and they were found to be 2.63 Mg/m³, 80 GPa and 30 GPa respectively. The two lines in Figure 9 correspond to the elastic constants C_{11} and C_{22} of a unidirectionally fiber reinforced composite where direction 1 is the fiber long axis and direction 2 is a transverse direction. The data points correspond to the elastic constants and the effective reinforcement volume fraction assuming no porosity, averaged over specimens of the same type. Error bars for moduli and reinforcement volume fraction were calculated based on a standard deviation within MMCs of a particular type. The large deviation of the reinforcement content in MMC Type A (effective average ceramic content 39%) from the actual ceramic content in the freeze-cast ceramic preform (about 44%) and the considerable variation in density found between individual samples may be attributed to the presence of uninfiltred regions in the MMC as well as local variation in ceramic content due to large colony size. Based on the measured densities of the two MMC types and the densities of alumina and Al-12Si, the extent of uninfiltred regions in MMC Types A and B were found to be about 3 vol% and less than 1 vol% respectively. The longitudinal elastic constants lie below the theoretical estimations and the transverse elastic constants lie close to the line corresponding to C_{22} . The considerable stretch of the error bars for both longitudinal and transverse moduli below their theoretical estimations can be explained by the presence of pores in the ceramic reinforcement after sintering, which reduce their effective stiffness in comparison to the theoretical values. It is expected that porosity should affect C_{11} much more than C_{22} and this explains the larger discrepancy between the observed average C_{11} values and the theoretical estimations. Moreover, the cracks as mentioned above also reduce the

stiffness. These effects were not considered in the theoretical model used here for comparison.

In order to shed light on the elastic anisotropy of the lamellar domains, the individual lamella orientation of the single-domain samples of MMC Type A was taken into account. Assuming no porosity, the average ceramic content in these 12 samples was found to be 39 vol%. In Figure 10 the quantity ρV^2 is plotted against the angle β (where $\beta = \alpha$ for $V = V_2$ and $\beta = (90-\alpha)$ for $V = V_3$). The ordinate values obtained from two extremes of the plot (corresponding to $\beta = 0^\circ$ and $\beta = 90^\circ$) are the elastic constants C'_{33} and C'_{22} of the lamellar domains in the domain coordinate system, where direction 2' is perpendicular to the lamellar plane and direction 3' is parallel to it. C'_{33} is about 215 GPa and C'_{22} is about 165 GPa. The third elastic constant, C'_{11} , is simply obtained from the average velocities V_1 of the single-domain samples. The result for this elastic constant is $C'_{11} = 230$ GPa and as expected this is close to the C'_{33} in Figure 11 corresponding to $\beta = 0$. The stiffness range defined by the highest and the lowest of these three elastic constants, C'_{11} and C'_{22} , is similar to the interval defined by the fiber models described above.

Torquato [Chapter 16 in 25] has compiled the theoretical model to estimate the transverse isotropic stiffness matrix for a rank 1 laminate composite consisting of alternating layers of phases of random thickness. With the help of this model and using the elastic constants and the effective volume fractions of alumina and Al-12Si, theoretical estimations for $C'_{11} = C'_{22}$ and for C'_{33} were calculated. Until this point the theoretical estimation of C'_{22} and C'_{33} used the assumption that direction 1 was always the freezing direction of the preform and the angle β was either 0° or 90° . To calculate the elastic constant for any intermediate angle β (where $0 \leq \beta \leq 90$), the laminate has to

be rotated about the 1-axis by the same angle. The expression for the corresponding transformed modulus is summarized by Berthelot [Table 11.1 in 22] and for the material under study this can be written as:

$$C_{33,\beta} = C_{33} \cos^4 \beta + C_{22} \sin^4 \beta + 2(C_{23} + 2C_{44}) \sin^2 \beta \cos^2 \beta \quad (\text{Eq. 3})$$

where $C'_{33,\beta}$ is the transformed elastic constant and C'_{22} , C'_{33} , C'_{23} and C'_{44} are calculated from the model compiled by Torquato. The result is plotted in Fig. 10 as the dashed curve. It shows that the predictions at small β are significantly higher than the experimental observations, while the fit is much better at high β values. A better match between theory and experiments is obtained assuming a value of 330 GPa for the Young's modulus of alumina. This underlines our previous assumption that the pores present within the ceramic region affect the elastic constant C'_{33} (parallel to the composite layers) much more than C'_{22} (perpendicular to the composite layers).

The pronounced anisotropy on the length scale of individual domains is of interest for further studies on the mechanics of poly-domain material because this anisotropy will create stress concentrations at domain boundaries. The results of the present study suggest that unidirectional fiber model can be used to yield a first estimate of the selected elastic constants for poly domain samples. Still, for a deeper analysis it may be required to also include models for layered materials to correlate the behavior of individual domains. .

4. Conclusions

Innovative metal matrix composites (MMC) produced by melt infiltration of ceramic preforms prepared by a freeze casting technique were examined. These composites exhibit lamellar domains with sizes up to several millimetres, composed of

alternating ceramic and metallic lamellae with thicknesses ranging from 20 to 100 μm . The elastic properties of the MMC were analyzed on samples of two different size classes, representing either poly-domain or single-domain behaviour. Results show that the individual domains exhibit a pronounced elastic anisotropy. The highest stiffness is observed in the direction parallel to the preform freezing direction, the lowest in the direction perpendicular to it. The elastic constants determined based on the effective ceramic content (assuming no porosity) lie within and near the bounds set by models established for unidirectionally fiber reinforced composites. The elastic anisotropy of individual domains is of interest for further studies on the mechanics of poly-domain material because this anisotropy will create stress concentrations at domain boundaries.

Acknowledgements

We thank M.J. Hoffmann, R. Oberacker, and T. Waschkies of Insitut für Keramik im Maschinenbau, Universität Karlsruhe, as well as A. Nagel and co-workers at Aalen University of Applied Sciences, Aalen, Germany, for providing the specimen material. We also thank Mr. Jared Bulach for his assistance in performing the ultrasonic experiments. Financial support from Deutsche Forschungsgemeinschaft (DFG), Bonn, Germany under project Wa1122/3-1 is gratefully acknowledged.

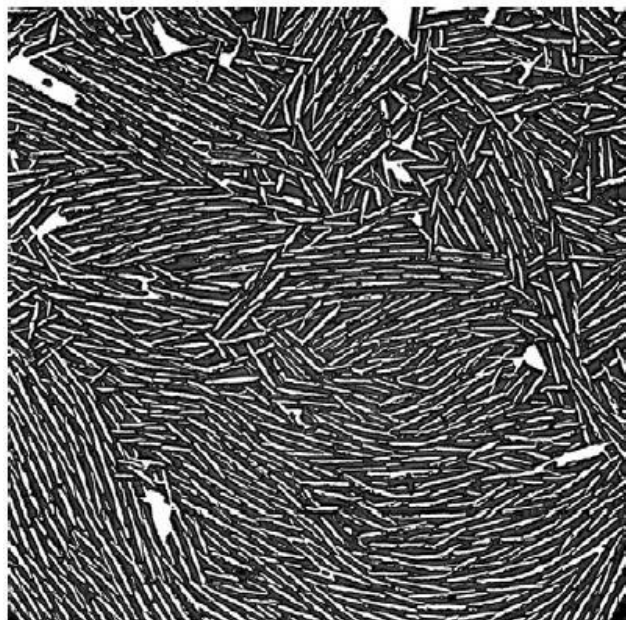
Figure captions

- Fig. 1: Microstructures of the MMCs for the faces perpendicular to the freezing direction of the preform (a) MMC Type A and (b) MMC Type B
- Fig. 2: Microstructures of the MMCs for the faces parallel to the freezing direction of the preform (a - b) MMC Type A and (c-d) MMC Type B
- Fig. 3: Schematic of the specimen co-ordinate system employed for ultrasound analysis
- Fig. 4: Definition of the angle α , marking the orientation of the single domain MMC specimen with respect to direction 2 of the specimen coordinate system.
- Fig. 5: Typical phase and amplitude spectra obtained from ultrasonic analysis on (a) single-domain and (b) poly-domain samples of MMC Type A
- Fig. 6: Plot showing the variation of wave velocity along the freezing direction of the freeze-casting preforms with specimen density for the poly-domain MMC samples
- Fig. 7: Plot showing the variation of wave velocity along the directions transverse to the freezing direction of the freeze casting preforms with specimen density for poly-domain MMC samples
- Fig. 8: Structure of the plane perpendicular to the freezing direction for a single-domain sample of MMC Type A showing the presence of a crack
- Fig. 9: Correlation of the average results obtained from ultrasonic analysis with the theoretical models for UD fiber reinforced composites
- Fig. 10: Effect of domain orientation on the quantity ρV^2 for single-domain specimens of MMC Type A

Table 1: Average densities and elastic constants of poly-domain MMCs. The elastic constants were determined from the average densities and average wave velocities.

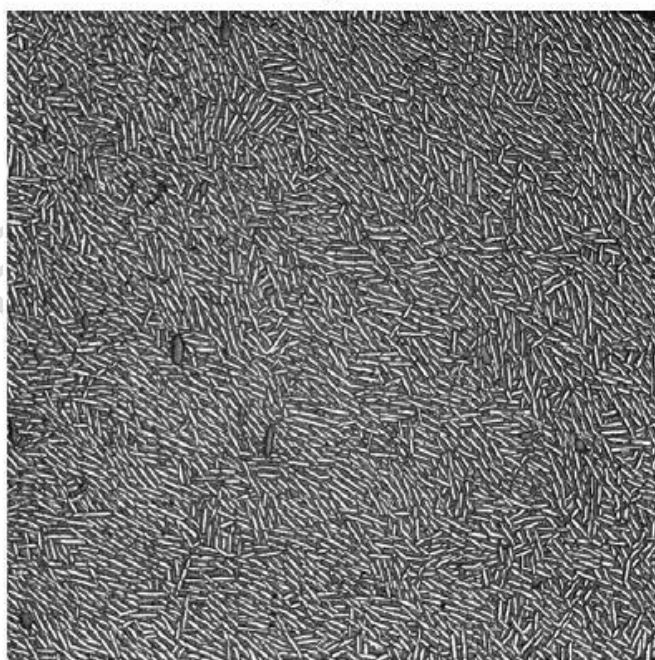
Specimens	Average density	Average of velocities V_1	Average of velocities V_2	Average of velocities V_3	Average elastic constant C_{11}	Average elastic constants $C_{22}=C_{33}$
	(Mg/m ³)	(m/s)	(m/s)	(m/s)	(GPa)	(GPa)
MMC Type A	3.12 ± 0.03	8354 ± 242	7637 ± 307	7366 ± 366	218 ± 14	176 ± 17
MMC Type B	3.18 ± 0.04	8685 ± 179	7669 ± 244	7824 ± 307	240 ± 10	192 ± 13

a)



2 mm

b)



2 mm

Fig. 1:

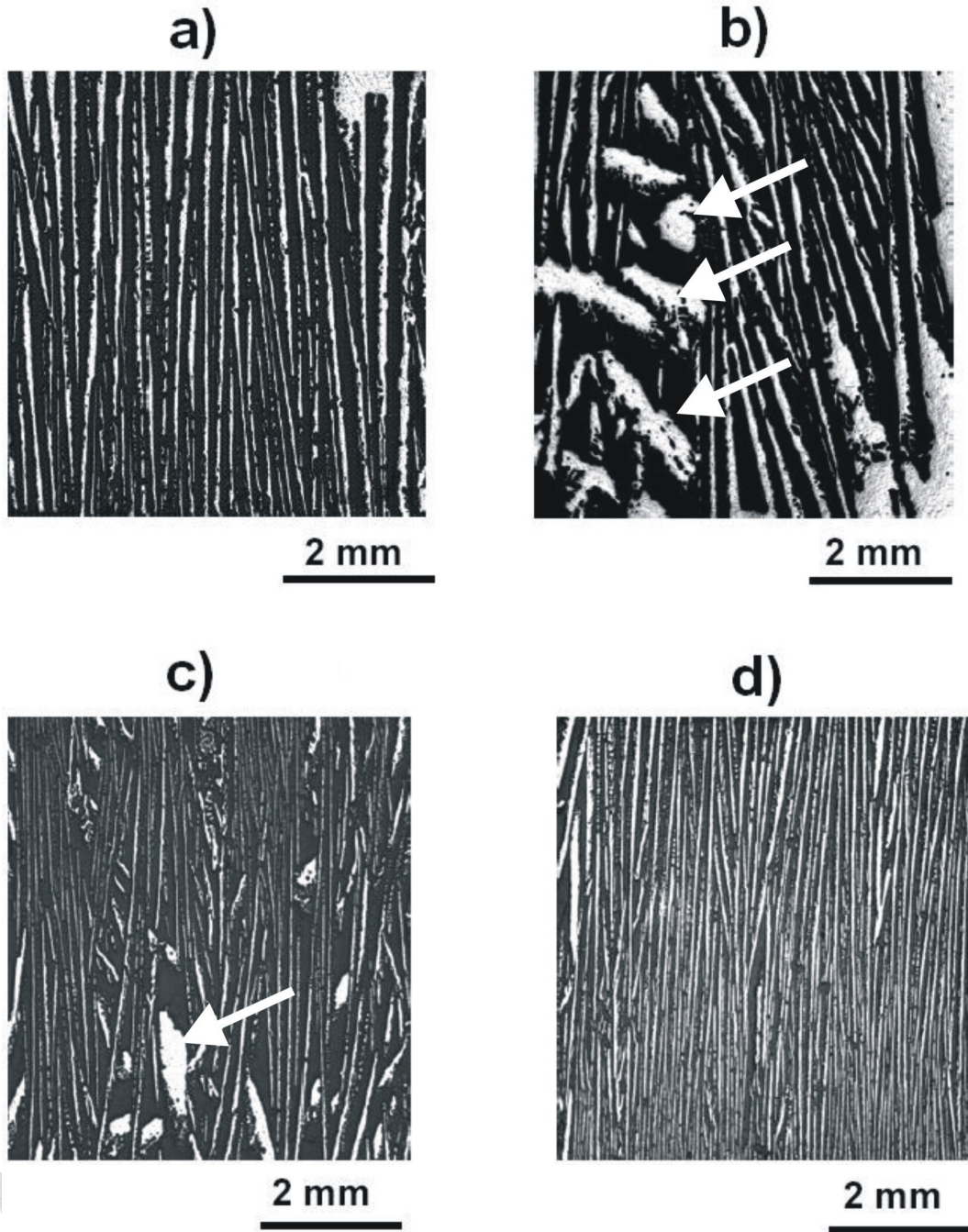


Fig. 2:

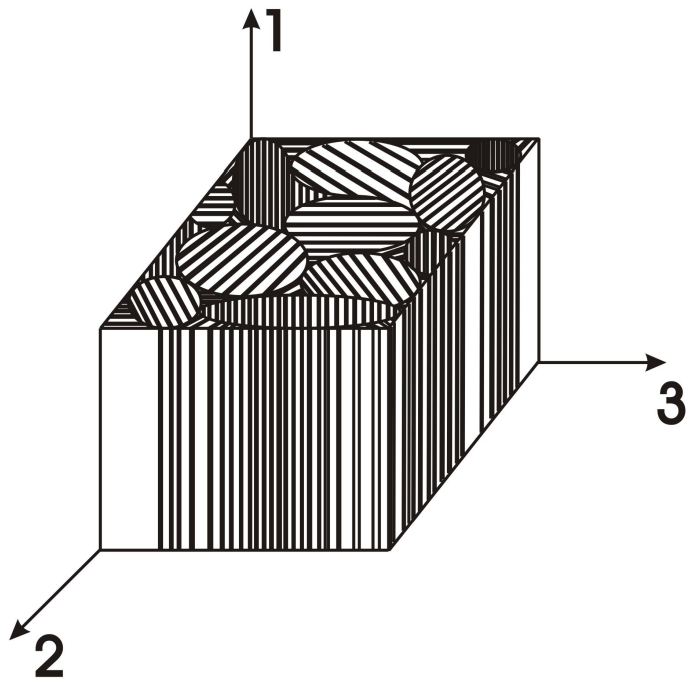


Fig. 3:

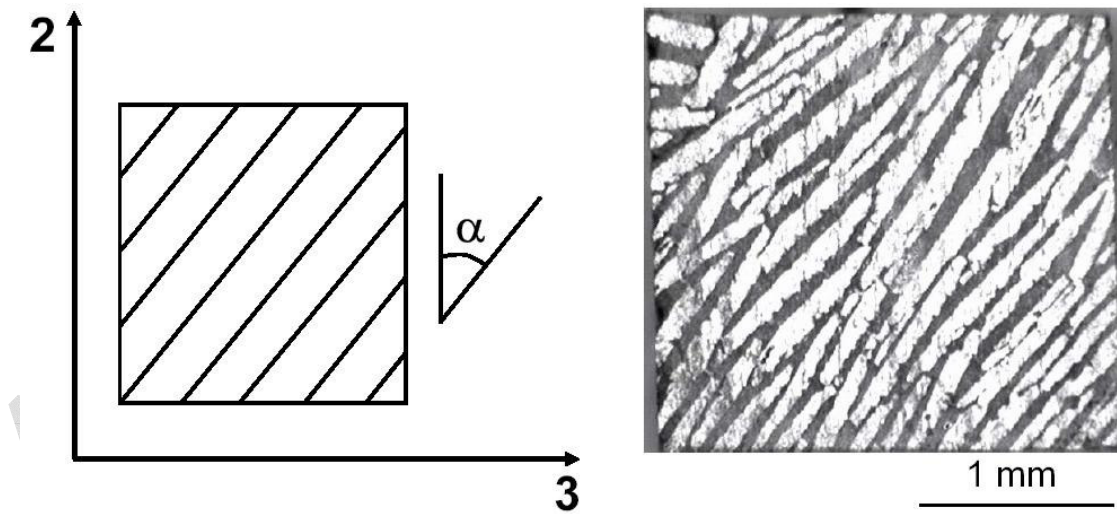


Fig. 4:

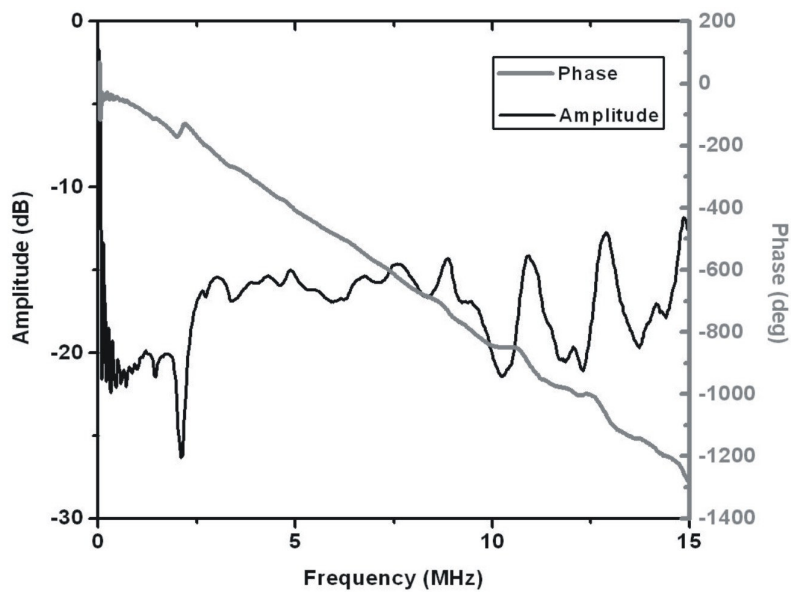
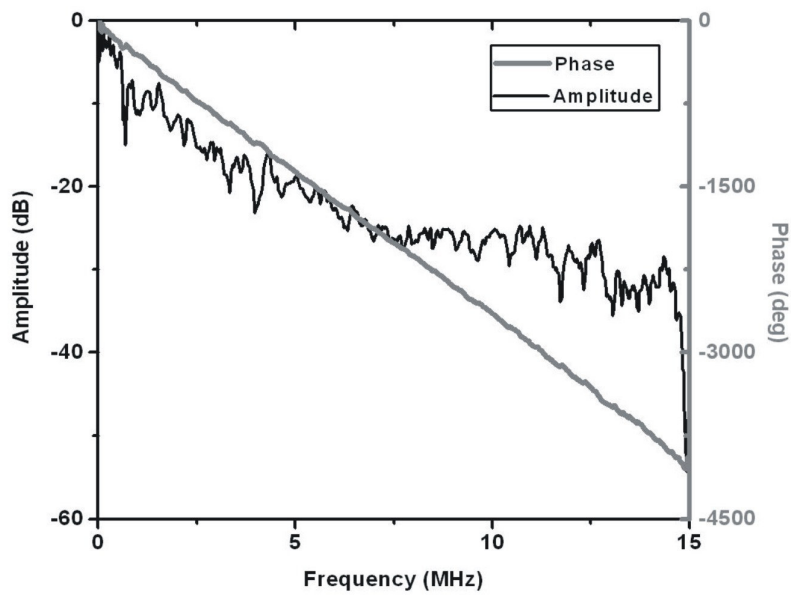
a)**b)**

Fig. 5:

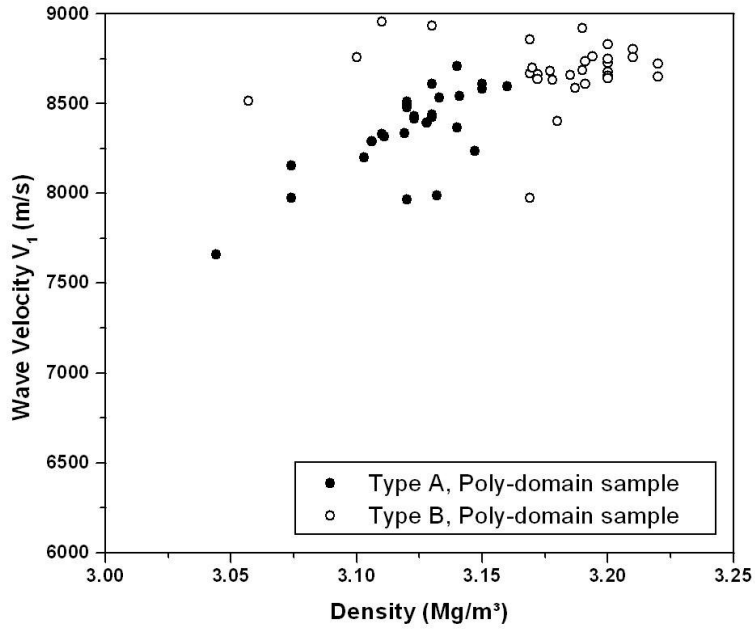


Fig. 6:

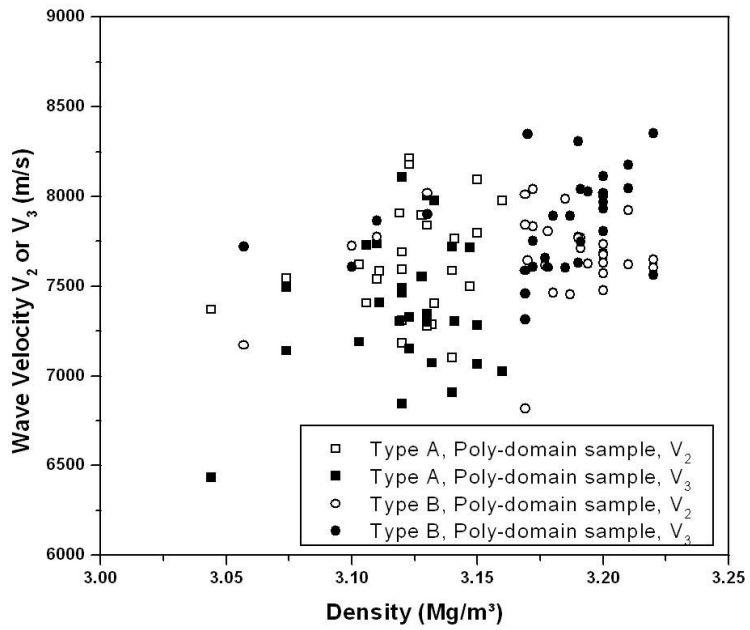


Fig. 7:



Fig. 8:

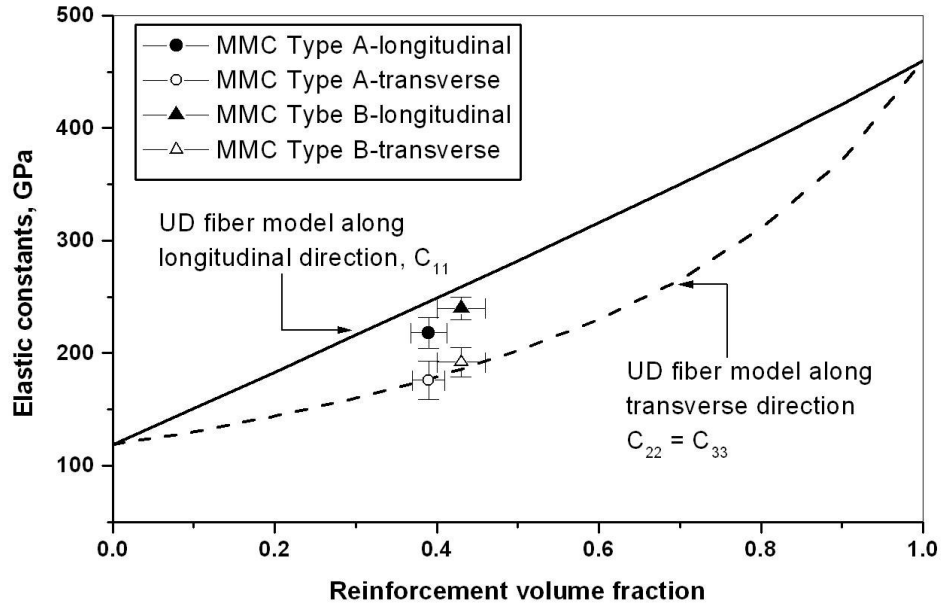


Fig. 9

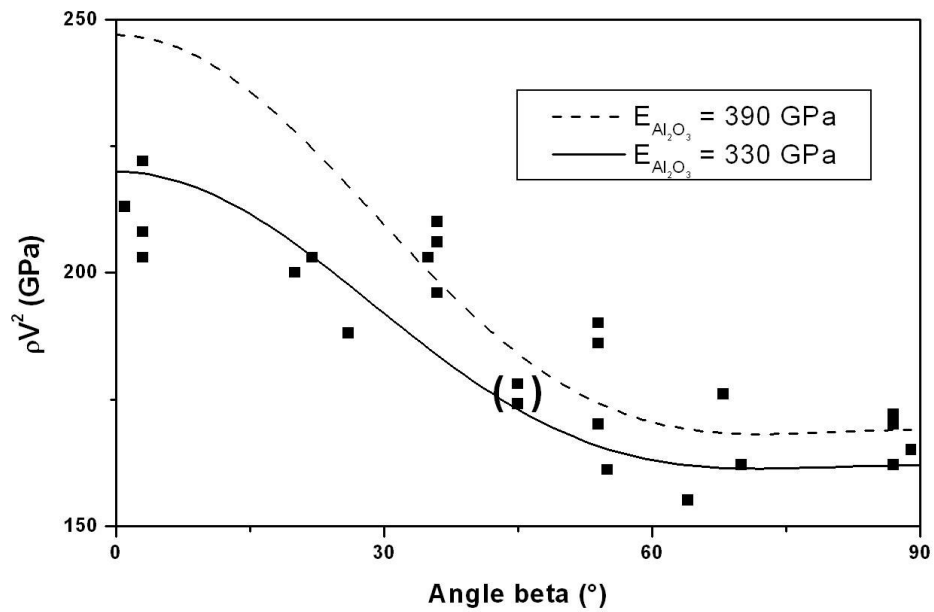


Fig. 10

References

1. Chawla N, Chawla KK. Metal Matrix Composites. Springer; 2006
2. Clyne TW, Withers PJ. An Introduction to Metal Matrix Composites. Cambridge: Cambridge University Press; 1993
3. Jones RM. Mechanics of Composite Materials. Taylor & Francis; 1999
4. Berthelot J-M. Composite Materials: Mechanical Behavior and Structural Analysis. Springer; 1999, Chapter 1
5. Mattern A. Interpenetrierende Metall-Keramik-Verbundwerkstoffe mit isotropen und anisotropen Al₂O₃-Verstärkungen (Interpenetrating metal-ceramic composites with isotropic and anisotropic Al₂O₃ Reinforcement.), Doctoral Thesis (in German), Universität Karlsruhe (TH), Karlsruhe, Germany. Full text appeared in: Schriftenreihe des Instituts für Keramik im Maschinenbau, ISSN 1436-3488, Vol. 44, 2005.
6. Fukasawa T, Deng Z-Y, Ando M, Ohji T, Kanzaki S. Synthesis of porous silicon nitride with unidirectionally aligned channels using freeze drying process. Journal of American ceramic Society 2002; 85(9): 2151-2155
7. Sofie SW, Dogan F. Freeze casting of aqueous alumina slurries with glycerol. Journal of American ceramic Society 2001; 84(7): 1459-1464
8. Fukasawa T, Ando M, Ohji T, Kanzaki S. Synthesis of porous ceramics with complex pore structure by freeze-dry processing. Journal of American ceramic Society 2001; 84(1): 230-232
9. Koh Y-H, Sun J-J, Kim H-E, Freeze casting of porous Ni-YSZ cermets, Materials Letters 2007; 61: 1283-1287
10. Deville S, Saiz E, Nalla RK, Tomsia AP. Freezing as a part to build complex composites. Science 2006; 311: 515-518
11. Deville S, Saiz E, Tomsia AP. Ice-templated porous alumina structures. Acta Materialia 2007; 55: 1965-1974
12. Ghomashchi MR, Vikhrov A. Squeeze casting: an overview. Journal of Materials Processing Technology 2000; 101: 1-9
13. Clyne TW, Mason JF. The squeeze infiltration process for fabrication of metal-matrix composites. Metallurgical Transactions A 1987; 18A: 1519-1530
14. Lloyd DJ. Particle reinforced aluminium and magnesium matrix composites. International Materials reviews 1994; 39: 1-23
15. Skirl S, Hoffman M, Bowman K, Wiederhorn S, Rödel J. Thermal expansion behavior and macrostrain of Al₂O₃/Al composites with interpenetrating networks. Acta Materialia 1998; 46: 2493-2499
16. Prielipp H, Knechtel M, Claussen N, Streiffner SK, Müllejans H, Rühle M, Rödel J. Strength and fracture toughness of aluminum/alumina composites with interpenetrating networks. Materials Science and Engineering 1995; A197: 19-30
17. Schreiber E, Anderson OL, Soga N. Elastic Constants and Their Measurement, McGraw-Hill, Inc., 1973
18. Wanner A. Elastic modulus measurements of extremely porous ceramic materials by ultrasonic phase spectroscopy. Materials Science and Engineering 1998; A248: 35-43
19. Papadakis EP. Ultrasonic velocity and attenuation: measurement methods with scientific and industrial applications. Physical Acoustics 1976; 12: 277-375
20. Papadakis EP. Ultrasonic diffraction from single apertures with application to pulse measurements and crystal physics. Physical Acoustics 1975; 18: 151-209
21. Lynnworth LC, Papadakis EP, Rea WR. Ultrasonic measurement of phase and group velocity using continuous wave transmission techniques. Final Report – Contract DAAG46-72-C-0186, Army Materials and Mechanics Research Center, Watertown, Massachusetts, Jan 1973
22. Berthelot JM, Composite Materials – Mechanical Behaviour and Structural Analysis, Springer, 1999,
23. Engineered Materials Handbook. Vol 1. Composites. ASM International; 1987
24. Materials Science and Engineering Handbook. CRC Press; 2001
25. Torquato S, Random Heterogeneous materials Microstructure and Macroscopic Properties, Springer, 2002